A Study on Source-Relay Cooperation for the Outage-constrained Relay Channel

Marcin Iwanow[12], Andreas Gründinger[2], Michael Joham,[2] and Wolfgang Utschick[2]
[1]Huawei Technologies Düsseldorf GmbH, Munich, Germany
Email: marcin.iwanow@tum.de
[2]Fachgebiet Methoden der Signalverarbeitung Technische Universität München, Germany
Email: {gruendinger, joham, utschick}@tum.de

***Abstract*—We study the influence of source-relay cooperation on the outage-constrained capacity bounds of the Gaussian relay channel. As was observed, coherent source-relay transmission does not lead to improvement for the *decode and forward* (DF) achievable rate in the presence of Rayleigh fading. We show that this is in sharp contrast to the case with known channel means. Then, transmission gains highly from coherent source-relay to destination transmission.**

I. Introduction

The general concept of relaying was introduced by van der Meulen in [1]. Until now, the general expression for the capacity of the relay channel is not known. An important contribution on the information-theoretic investigation of the relay channel was given by Cover and El Gamal in [2]. They provided upper and lower bounds for the capacity. Among others, the *decode-and-forward* (DF) strategy and the *cut-set-bound* (CSB) were defined to bound the capacity from below and above, respectively.

In our study, we consider a full-duplex system and assume that only the receiving nodes have full *channel state information* (CSI) while the transmitting nodes have only access to the channels' statistics. The approach for evaluating the systems' performance under such conditions varies upon the assumed fading model. In this work, we assume slow fading of the channel and, therefore, we investigate the outage capacity of the relay channel [3].

Bounds on the outage probability of the relay channel have been studied by Kramer et al. in [4] for a full-duplex setup and phase fading with a given rate. Høst-Madsen and Zhang extended the results to a half-duplex setup in [5]. Other works, e.g., [6], [7], focused their study on low-SNR regions.

Similar to [8], we consider the reverse problem, namely deriving rate bounds for a restricted outage probability. This work extends the results from the aforementioned paper and provides a detailed discussion about the question when source-relay cooperation is advantageous and supports communication.

While the work in [8] concentrated on the Rayleigh channel model, in this paper, we assume a *line of sight* (LOS) component for the channel distribution, i.e., a *Rician fading* model.

The analysis of the Gaussian relay channel in [8] assured, that the DF strategy does not benefit from cooperation between the relay and the source if Rayleigh channels between the terminals are assumed. In particular, coherent source-relay transmission does not result in increased DF rate for a small outage requirement. The aim of our study is to show that the situation is different for known channel mean and single/multiple antennas at the relay terminal. For a wide class of such channels, cooperation leads to gains in the outage-constrained DF rates.

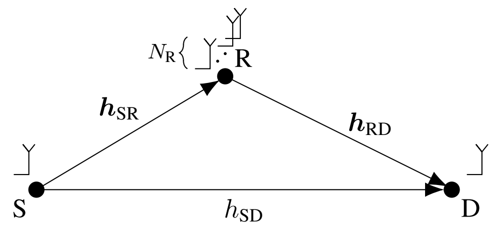

Fig. 1. Setup with multi-antenna relay

In the remainder of the paper, we introduce the model of the system, motivate the research and present our contribution together with the simulative results.

II. System Model

We assume a three-node Gaussian relay system as shown in Fig. 1. The investigations are for a setup with single-antenna source and destination and with $N_{\mathrm{R}} \geq 1$ antennas at the relay.

The signals received at the relay and destination read as

$$\begin{aligned} \boldsymbol{y}_{\mathrm{R}} &= \boldsymbol{h}_{\mathrm{SR}} x_{\mathrm{S}} + \boldsymbol{n}_{\mathrm{R}}, \\ y_{\mathrm{D}} &= h_{\mathrm{SD}} x_{\mathrm{S}} + \boldsymbol{h}_{\mathrm{RD}}^{\mathrm{H}} \boldsymbol{x}_{\mathrm{R}} + n_{\mathrm{D}}. \end{aligned} \tag{1}$$

The noise components are independent of each other as well as of the transmitter signals with $\boldsymbol{n}_{\mathrm{R}} \sim \mathcal{N}_{\mathbb{C}}(\mathbf{0}, \mathbf{I}), n_{\mathrm{D}} \sim \mathcal{N}_{\mathbb{C}}(0, 1)$. Without loss of generality and optimality, we assume zero-mean channel inputs x_{S} and $\boldsymbol{x}_{\mathrm{R}}$ constrained with the available power budget $\mathrm{E}[|x_{\mathrm{S}}|^2] \leq P_{\mathrm{S}}$ and $\mathrm{E}[\|\boldsymbol{x}_{\mathrm{R}}\|_2^2] \leq P_{\mathrm{R}}$.

In our work, we provide results for a channel model with known mean. For example, we assume one direct path and multiple scattered paths. Omitting the subscripts referring to the links, the formal description reads as

$$\boldsymbol{h} = \bar{\boldsymbol{h}} + \hat{\boldsymbol{h}}, \quad \hat{\boldsymbol{h}} \sim \mathcal{N}_{\mathbb{C}}(\mathbf{0}, \sigma_{\hat{\boldsymbol{h}}}^2 \mathbf{I}). \tag{2}$$

The Rician K factor is defined as the ratio of the power of the direct path and the power of the scatterers $K = \frac{|[\bar{\boldsymbol{h}}]_i|^2}{\sigma^2_{\tilde{\boldsymbol{h}}}}\ \forall i$, where $[\bar{\boldsymbol{h}}]_i$ stands for the $i-$th entry of the direct path channel vector $\bar{\boldsymbol{h}}$. Additionally we assume that $\sigma^2_{\boldsymbol{h}} = \mathrm{E}\left[|[\boldsymbol{h}]_i|^2\right]$ constant for each i.

We see the extension of the analysis in [8] to the channels in (2) as an important input to the discussion on practical applications of relaying systems. For example, in mmWave systems, which are considered to be included in the 5G standards, it is agreed that a strong LOS path is required for maintaining connectivity between the terminals.

III. Problem statement

Capacity bounds for the relay channel with perfect CSI were given by Cover and El Gamal in [2]. Gaussian full-power signaling maximizes the DF achievable rate as well as the CSB expression for the Gaussian relay channel. Thus, the DF rate and CSB expression can be written as (cf. [8])

$$C_{\text{CSB}}(\boldsymbol{h}) = \max_{\beta} \min \left\{ C^{(1)}_{\text{CSB}}(\beta, \boldsymbol{h}), C^{(2)}_{\text{CSB}}(\beta, \boldsymbol{h}) \right\}, \quad (3)$$

$$R_{\text{DF}}(\boldsymbol{h}) = \max_{\beta} \min \left\{ R^{(1)}_{\text{DF}}(\beta, \boldsymbol{h}), R^{(2)}_{\text{DF}}(\beta, \boldsymbol{h}) \right\} \quad (4)$$

where

$$C^{(1)}_{\text{CSB}}(\beta, \boldsymbol{h}) = \log_2 \left(1 + (1 - g(\beta)) \left(\|\boldsymbol{h}_{\text{SR}}\|_2^2 + |h_{\text{SD}}|^2\right) P_{\text{S}}\right), \quad (5)$$

$$R^{(1)}_{\text{DF}}(\beta, \boldsymbol{h}) = \log_2 \left(1 + (1 - g(\beta)) \|\boldsymbol{h}_{\text{SR}}\|_2^2 P_{\text{S}}\right), \quad (6)$$

$$C^{(2)}_{\text{CSB}}(\beta, \boldsymbol{h}) = R^{(2)}_{\text{DF}}(\beta, \boldsymbol{h}) = = \log_2 \left(1 + [h^*_{\text{SD}}, \boldsymbol{h}^{\text{H}}_{\text{RD}}] \boldsymbol{C} [h_{\text{SD}}, \boldsymbol{h}^{\text{T}}_{\text{RD}}]^{\text{T}}\right), \quad (7)$$

where the matrix

$$\boldsymbol{C} = \begin{bmatrix} P_{\text{S}} & \beta\sqrt{P_{\text{S}}P_{\text{R}}}\frac{\boldsymbol{r}^{\text{H}}_{\text{SR}}}{\|\boldsymbol{r}_{\text{SR}}\|_2} \\ \beta\sqrt{P_{\text{S}}P_{\text{R}}}\frac{\boldsymbol{r}_{\text{SR}}}{\|\boldsymbol{r}_{\text{SR}}\|_2} & \boldsymbol{R}_{\text{R}} \end{bmatrix} \quad (8)$$

is the joint covariance matrix of the source and the relay, $\beta \in [0, 1]$, $\boldsymbol{R}_{\text{R}} = \mathrm{E}[\boldsymbol{x}_{\text{R}}\boldsymbol{x}^{\text{H}}_{\text{R}}]$ is the covariance matrix of the relay, $\boldsymbol{r}_{\text{SR}} = \mathrm{E}[\boldsymbol{x}_{\text{R}}x^*_{\text{S}}]$, and $g(\beta) = \beta^2 \frac{P_{\text{R}}\boldsymbol{r}^{\text{H}}_{\text{SR}}\boldsymbol{R}^{\dagger}_{\text{R}}\boldsymbol{r}_{\text{SR}}}{\|\boldsymbol{r}_{\text{SR}}\|_2^2} \in [0, 1]$. The formula for $g(\beta)$ stems from the expression for the conditional covariance $\mathrm{cov}(x_{\text{S}}|\boldsymbol{x}_{\text{R}}) = P_{\text{S}} - \boldsymbol{r}^{\text{H}}_{\text{SR}}\boldsymbol{R}^{\dagger}_{\text{R}}\boldsymbol{r}_{\text{SR}}$ where $(\cdot)^{\dagger}$ denotes the Moore-Penrose pseudoinverse [9].

Both, the CSB expression in (3) and the DF rate in (4), can be seen as the minimum rate of two links. In the first link, the source is transmitting and either the relay and destination are jointly receiving (for the CSB) or only the relay is receiving (for the DF). In the second link (for both CSB and DF), the source and relay are jointly transmitting and the destination terminal serves as the receiver. In our work, we place emphasis on the analysis of the joint source-relay transmission. The degree of cooperation is modeled by β and the specifics of the cooperation is included in $\boldsymbol{r}_{\text{SR}}$.

As pointed out in the introduction, we focus on setups with imperfect channel knowledge and the outage capacity as performance measure. Therefore, we define the DF rate bound and CSB on the ε-outage capacity as

$$R^{(\text{out})}_{\text{DF}} = \max_{\rho,\beta} \left\{\rho \in \mathbb{R} : \ p_{\text{DF}}(\rho, \beta) \geq 1 - \varepsilon\right\}, \quad (9)$$

$$C^{(\text{out})}_{\text{CSB}} = \max_{\rho,\beta} \left\{\rho \in \mathbb{R} : \ p_{\text{CSB}}(\rho, \beta) \geq 1 - \varepsilon\right\} \quad (10)$$

where the probabilities inside (9) and (10) are defined as

$$p_{\text{DF}}(\rho, \beta) = \Pr\left[\min_{i=1,2}\left\{R^{(\text{i})}_{\text{DF}}(\beta, \boldsymbol{h})\right\} \geq \rho\right], \quad (11)$$

$$p_{\text{CSB}}(\rho, \beta) = \Pr\left[\min_{i=1,2}\left\{C^{(\text{i})}_{\text{CSB}}(\beta, \boldsymbol{h})\right\} \geq \rho\right]. \quad (12)$$

Both, (9) and (10), are chance-constrained optimization problems with unknown convexity properties. In [8], these problems are studied for a single-antenna at the relay terminal and Rayleigh fading channels. As mentioned, we consider the Rician fading channel model and extend the study to multi-antenna setups.

IV. Single-Antenna Relay

We investigate the impact of source-relay cooperation on the outage-constrained DF rate (4) first for the single relay antenna setup. To this end, we rewrite (7) as

$$R^{(2)}_{\text{DF}}(\beta, \boldsymbol{h}) = \log_2 \left(1 + |h_{\text{SD}}|^2 P_{\text{S}} + h_{\text{RD}}P_{\text{R}} + 2\mathrm{Re}(h^*_{\text{SD}}h_{\text{RD}}r_{\text{SR}})\right). \quad (13)$$

For perfect CSI, the r_{SR} that maximizes (4) is available in closed form and reads as

$$r_{\text{SR}} = \sqrt{P_{\text{S}}P_{\text{R}}}\frac{h^*_{\text{SD}}h_{\text{RD}}}{|h_{\text{SD}}||h_{\text{RD}}|}\beta \quad (14)$$

where the optimal β leads to equal $R^{(1)}_{\text{DF}}(\beta, \boldsymbol{h})$ and $R^{(2)}_{\text{DF}}(\beta, \boldsymbol{h})$, if possible. Thus, the non-coherent transmission maximizes the first rate expression since $R^{(1)}_{\text{DF}}(\beta, \boldsymbol{h})$ only depends on β^2 and (genie-aided) coherent transmission maximizes the second rate expression. The situation becomes less obvious, when only the channel statistics are available. Then, if we heuristically model the cross-covariance as

$$r_{\text{SR}} = \sqrt{P_{\text{S}}P_{\text{R}}}\frac{\bar{h}^*_{\text{SD}}\bar{h}_{\text{RD}}}{|\bar{h}_{\text{SD}}||\bar{h}_{\text{RD}}|}\beta, \quad (15)$$

the expression $\mathrm{Re}(h^*_{\text{SD}}h_{\text{RD}}r_{\text{SR}})$ can be less than zero for certain channel realizations. We note that the probability of this event increases with decreasing Rician K-factor. The limit case, i.e., with K equal to zero results in Rayleigh fading channels. For this channel, we know from [8] that non-coherent transmission is optimal. On the other hand, for K equal to infinity, we know that the channel is perfectly known and, thus, the transmission always profits from cooperation. We expect that we will benefit in various degrees from the source-relay cooperation for Rician K-factors in between. We provide the results of the Monte-Carlo simulations and discussion upon in Section IX.

V. Multi-antenna Relay

Next, we consider the multi-antenna relay setup. The source-relay cooperation is then modeled with the vector $\boldsymbol{r}_{\mathrm{SR}}$ and the relay transmit strategy is defined by the relay covariance matrix $\boldsymbol{R}_{\mathrm{R}}$. For perfect CSI, the $\boldsymbol{r}_{\mathrm{SR}}$ and $\boldsymbol{R}_{\mathrm{R}}$ that maximize (7) are given in closed form by

$$\boldsymbol{r}_{\mathrm{SR}} = \sqrt{P_{\mathrm{S}}P_{\mathrm{R}}}\frac{h_{\mathrm{SD}}^{*}\boldsymbol{h}_{\mathrm{RD}}}{|h_{\mathrm{SD}}|\|\boldsymbol{h}_{\mathrm{RD}}\|_2}\beta, \tag{16}$$

$$\boldsymbol{R}_{\mathrm{R}} = \frac{\boldsymbol{h}_{\mathrm{RD}}\boldsymbol{h}_{\mathrm{RD}}^{\mathrm{H}}}{\|\boldsymbol{h}_{\mathrm{RD}}\|_2^2}P_{\mathrm{R}} \tag{17}$$

where the optimal β leads to equal $R_{\mathrm{DF}}^{(1)}(\beta,\boldsymbol{h})$ and $R_{\mathrm{DF}}^{(2)}(\beta,\boldsymbol{h})$, if possible.

If only the channel statistics are available, we follow the strategy from Section IV and model $\boldsymbol{r}_{\mathrm{SR}}$ heuristically as

$$\boldsymbol{r}_{\mathrm{SR}} = \sqrt{P_{\mathrm{S}}P_{\mathrm{R}}}\frac{\bar{h}_{\mathrm{SD}}^{*}\bar{\boldsymbol{h}}_{\mathrm{RD}}}{|\bar{h}_{\mathrm{SD}}|\|\bar{\boldsymbol{h}}_{\mathrm{RD}}\|_2}\beta. \tag{18}$$

We investigate the system performance for two relay transmit strategies. In the first one, we match $\boldsymbol{R}_{\mathrm{R}}$ to the channel mean $\bar{\boldsymbol{h}}_{\mathrm{RD}}$, i.e.,

$$\boldsymbol{R}_{\mathrm{R}} = \frac{\bar{\boldsymbol{h}}_{\mathrm{RD}}\bar{\boldsymbol{h}}_{\mathrm{RD}}^{\mathrm{H}}}{\|\bar{\boldsymbol{h}}_{\mathrm{RD}}\|_2^2}P_{\mathrm{R}}. \tag{19}$$

In the second one, we set the covariance matrix to a scaled identity matrix

$$\boldsymbol{R}_{\mathrm{R}} = \frac{P_{\mathrm{R}}}{N_{\mathrm{R}}}\mathbf{I}. \tag{20}$$

In this case, we additionally scale $\boldsymbol{r}_{\mathrm{SR}}$ by $1/\sqrt{N_{\mathrm{R}}}$, in order to assure that $\boldsymbol{C}$ remains positive-semidefinite:

$$\boldsymbol{r}_{\mathrm{SR}} = \sqrt{\frac{P_{\mathrm{S}}P_{\mathrm{R}}}{N_{\mathrm{R}}}}\frac{\bar{h}_{\mathrm{SD}}^{*}\bar{\boldsymbol{h}}_{\mathrm{RD}}}{|\bar{h}_{\mathrm{SD}}|\|\bar{\boldsymbol{h}}_{\mathrm{RD}}\|_2}\beta. \tag{21}$$

In Section IX, we provide Monte-Carlo simulations and discussion on the different transmission and cooperation designs.

VI. Decode-and-Forward Outage Rate Approximation

In this section, we provide an approximation to the ε-outage-constrained DF rate. We reformulate the optimization problem in (9) in order to obtain a tractable problem.

First, we observe that due to the independence of the channels, the expressions $R_{\mathrm{DF}}^{(1)}(\beta,\boldsymbol{h})$ and $R_{\mathrm{DF}}^{(2)}(\beta,\boldsymbol{h})$ are also independent. We can thus write the outage-constrained DF rate in (11) as

$$\begin{aligned} p_{\mathrm{DF}}(\rho,\beta) &= \Pr\left(R_{\mathrm{DF}}^{(1)}(\beta,\boldsymbol{h}) \geq \rho\right)\Pr\left(R_{\mathrm{DF}}^{(2)}(\beta,\boldsymbol{h}) \geq \rho\right) \\ &\triangleq p_{\mathrm{DF}}^{(1)}(\rho,\beta)p_{\mathrm{DF}}^{(2)}(\rho,\beta) = (1-\varepsilon_1)(1-\varepsilon_2). \end{aligned} \tag{22}$$

where $(\varepsilon_1,\varepsilon_2) \in [0,1]\times[0,1]$. Next we notice, that the inequality in (9) can be replaced by an equality, since $p_{\mathrm{DF}}(\rho,\beta)$ is non-increasing in ρ. Consequently, we rewrite (9) as

$$\begin{aligned} R_{\mathrm{DF}}^{(\mathrm{out})} = \max_{\rho,\beta,\gamma}\Big\{\rho\in\mathbb{R} : p_{\mathrm{DF}}^{(1)}(\rho,\beta) = 1-\varepsilon\frac{1-\gamma}{1-\gamma\varepsilon} \\ \wedge\, p_{\mathrm{DF}}^{(2)}(\rho,\beta) = 1-\gamma\varepsilon\Big\}. \end{aligned} \tag{23}$$

where we introduced $\gamma = \varepsilon_2/\varepsilon \in [0,1]$ and substituted ε_1 and ε_2 with $\varepsilon\frac{1-\gamma}{1-\gamma\varepsilon}$ and $\gamma\varepsilon$, respectively, such that $(1-\varepsilon_1)(1-\varepsilon_2) = 1-\varepsilon$.

In order to obtain $p_{\mathrm{DF}}^{(1)}(\rho,\beta)$ and $p_{\mathrm{DF}}^{(2)}(\rho,\beta)$, we analyze their explicit representation, i.e.,

$$p_{\mathrm{DF}}^{(1)}(\rho,\beta) = \Pr\left(\|\boldsymbol{h}_{\mathrm{SR}}\|_2^2 \geq \frac{2^{\rho}-1}{P_{\mathrm{S}}(1-g(\beta))}\right) \tag{24}$$

$$p_{\mathrm{DF}}^{(2)}(\rho,\beta) = \Pr\left([h_{\mathrm{SD}}^{*},\boldsymbol{h}_{\mathrm{RD}}^{\mathrm{H}}]\boldsymbol{C}[h_{\mathrm{SD}},\boldsymbol{h}_{\mathrm{RD}}^{\mathrm{T}}]^{\mathrm{T}} \geq 2^{\rho}-1\right). \tag{25}$$

The probability in (24) is given in a closed form (cf. Appendix A), as $\|\boldsymbol{h}_{\mathrm{SR}}\|_2^2$ is distributed with scaled non-central chi-squared distribution. On the other hand, the tail probability of a quadratic form in normal variables is not known in a closed form. Therefore, we propose to approximate $p_{\mathrm{DF}}^{(2)}(\rho,\beta)$ with help of one of the existing frameworks, e.g., [10], [11]. We denote the approximation with $p_{\mathrm{DF}}^{(2),\mathrm{app}}(\rho,\beta) \approx p_{\mathrm{DF}}^{(2)}(\rho,\beta)$.

Consequently, we can write (23) as following

$$R_{\mathrm{DF}}^{(\mathrm{out})} \approx \max_{\beta,\gamma}\left\{\min\left\{\rho_1(\beta,\gamma),\rho_2^{\mathrm{app}}(\beta,\gamma)\right\}\right\}. \tag{26}$$

where

$$\rho_1(\beta,\gamma) = \left\{\rho' : p_{\mathrm{DF}}^{(1)}(\rho',\beta) = 1-\varepsilon\frac{1-\gamma}{1-\gamma\varepsilon}\right\}, \tag{27}$$

$$\rho_2^{\mathrm{app}}(\beta,\gamma) = \left\{\rho' : p_{\mathrm{DF}}^{(2),\mathrm{app}}(\rho',\beta) = 1-\gamma\varepsilon\right\}. \tag{28}$$

We observe that in (26), the objective function is strictly unimodal in both β and γ. Although, it is not clear whether the function is unimodal jointly in both variables. In our simulations, we thus lower-bound the solution by solving the problem with the nested golden section search algorithm [12].

The problem in (27) can be solved, e.g., with the Newton's method and (28) with the bisection method.

In our simulations, we applied the approach from [10] for approximating $p_{\mathrm{DF}}^{(2)}(\rho,\beta)$. We have evaluated the precision of the approximations by comparison with the outcome of Monte-Carlo based simulations. The approximations turned out to be very precise – the curves were practically indistinguishable. Therefore, we omit plotting the comparison results in Section IX.

VII. Upper bound for the CSB

In this paper, we present one approach for upper-bounding the CSB expression in (3). Alike in [13], we loosen the CSB expression by upper bounding $C_{\mathrm{CSB}}^{(1)}(\beta,\boldsymbol{h})$ and $C_{\mathrm{CSB}}^{(2)}(\beta,\boldsymbol{h})$. Next, we find the probability $p_{\mathrm{LOS}}(\rho,\mu)$ that

$$C_{\mathrm{CSB}}^{(\mathrm{out})} \leq C_{\mathrm{LOS}}^{(\mathrm{out})} = \max_{\rho}\min_{\mu\geq 0}\left\{\rho\in\mathbb{R} : p_{\mathrm{LOS}}(\rho,\mu) \geq 1-\varepsilon\right\}, \tag{29}$$

where μ is an auxiliary variable and the inner minimization over it aims on tightening the bound.

The single-antenna case has been considered in [13]. It has been shown, that independent on the channel model, $p_{\mathrm{LOS}}(\rho,\mu)$ can be described as sum of probabilities of three disjoint events, that is,

$$p_{\mathrm{LOS}}(\rho,\mu) = p_{\mathrm{LOS}}^{(\mathrm{i})} + p_{\mathrm{LOS}}^{(\mathrm{ii})} + p_{\mathrm{LOS}}^{(\mathrm{iii})}. \tag{30}$$

For details we refer to [13]. In this paper, we provide only the intuitive description of the events:

(i) The source-destination link is able to hold the transmission of rate ρ with probability $1-\varepsilon$.
(ii) The source-destination link is not strong enough to convey the desired rate. Thus, the relay is required to "help".
(iii) The entire transmission has to be held through the relay.

The closed-form formulas for $p_{\text{LOS}}^{(\text{i})}$, $p_{\text{LOS}}^{(\text{ii})}$, and $p_{\text{LOS}}^{(\text{iii})}$ were derived for the Rayleigh channel model with single-antenna at the relay in [13].

In the upcoming sections, we provide the formulas for $p_{\text{LOS}}^{(\text{i})}$, $p_{\text{LOS}}^{(\text{ii})}$, and $p_{\text{LOS}}^{(\text{iii})}$ for the Rician channel model with single/multiple antennas present at the relay.

A. Single-antenna at the Relay

For the Rician channel model and only one antenna at the relay, we have

$$p_{\text{LOS}}^{(\text{i})} = 1-\mathcal{F}_{|h_{\text{SD}}|^2}\left(\frac{1}{P_{\text{S}}}k_0\right) \tag{31}$$

$$p_{\text{LOS}}^{(\text{ii})} = \int_{\frac{1}{P_{\text{S}}}k_1}^{\frac{1}{P_{\text{S}}}k_0} f_{|h_{\text{SD}}|^2}(x)\left(1-\mathcal{F}_{|h_{\text{SR}}|^2}\left(\frac{1}{P_{\text{S}}}k_0-x\right)\right)dx \tag{32}$$

$$p_{\text{LOS}}^{(\text{iii})} = \int_{0}^{\frac{1}{P_{\text{S}}}k_1} f_{|h_{\text{SD}}|^2}(x)\left(1-\mathcal{F}_{|h_{\text{RD}}|^2}\left(\frac{1}{P_{\text{R}}}(k_1-P_{\text{S}}x)\right)\right)dx \tag{33}$$

with

$$k_0 = 2^{\rho}-1 \tag{34}$$

$$k_1 = \frac{2^{\rho-\log_2\left(1+\frac{P_{\text{R}}}{\mu(P_{\text{S}}+P_{\text{R}})}\right)-\log_2\left(1+\frac{P_{\text{S}}}{\mu(P_{\text{S}}+P_{\text{R}})}\right)}-1}{\mu(P_{\text{S}}+P_{\text{R}})}. \tag{35}$$

We are not aware of closed-form expression for the expressions $p_{\text{LOS}}^{(\text{ii})}$ and $p_{\text{LOS}}^{(\text{ii})}$, therefore we apply numerical integration in our simulations.

B. Multiple Antennas at the Relay

With more than one antenna at the relay terminal, the bound for $C_{\text{CSB}}^{(2)}(\beta,\boldsymbol{h})$ from [13] does not hold any more. Here, we upper bound the $C_{\text{CSB}}^{(2)}(\beta,\boldsymbol{h})$ expression as follows

$$\begin{aligned}
C_{\text{CSB}}^{(2)} &\leq \log_2\det\left(\mathbf{I}+\frac{1}{\mu(P_{\text{R}}+P_{\text{S}})}\boldsymbol{C}\right)\\
&\quad+\log_2(1+\mu(P_{\text{S}}+P_{\text{R}})(|h_{\text{SD}}|^2+\|\boldsymbol{h}_{\text{RD}}\|_2^2))\\
&=\log_2\det\left(\mathbf{I}+\frac{1}{\mu(P_{\text{R}}+P_{\text{S}})}\boldsymbol{\Sigma}\right)\\
&\quad+\log_2(1+\mu(P_{\text{S}}+P_{\text{R}})(|h_{\text{SD}}|^2+\|\boldsymbol{h}_{\text{RD}}\|_2^2))\\
&\leq\log_2\det\left(\mathbf{I}+\frac{1}{\mu(P_{\text{R}}+P_{\text{S}})}\frac{P_{\text{R}}+P_{\text{S}}}{N_{\text{R}}+1}\mathbf{I}\right)\\
&\quad+\log_2(1+\mu(P_{\text{S}}+P_{\text{R}})(|h_{\text{SD}}|^2+\|\boldsymbol{h}_{\text{RD}}\|_2^2))\\
&=(N_{\text{R}}+1)\log_2\left(1+\frac{1}{\mu(N_{\text{R}}+1)}\right)\\
&\quad+\log_2(1+\mu(P_{\text{S}}+P_{\text{R}})(|h_{\text{SD}}|^2+\|\boldsymbol{h}_{\text{RD}}\|_2^2)).
\end{aligned} \tag{36}$$

The first inequality is a consequence of the theorem [14, Proof of Theorem 19.2]

$$\det(\mathbf{I}+\boldsymbol{A}\boldsymbol{B})\leq\det\left(\mathbf{I}+\frac{1}{\mu\text{tr}(\boldsymbol{A})}\boldsymbol{A}\right)\det(\mathbf{I}+\mu\text{tr}(\boldsymbol{A})\boldsymbol{B}) \tag{37}$$

where $\mu\geq 0$ and both $\boldsymbol{A}$ and $\boldsymbol{B}$ are complex positive-semidefinite matrices. We also exploit the fact that the eigenvalue decomposition of the positive-semidefinite matrix $\boldsymbol{C}$ can be written as $\boldsymbol{C}=\boldsymbol{U}\boldsymbol{\Sigma}\boldsymbol{U}^{\text{H}}$, where $\boldsymbol{U}$ is a unitary matrix.

Consequently, the probabilities $p_{\text{LOS}}^{(\text{i})}$, $p_{\text{LOS}}^{(\text{ii})}$, and $p_{\text{LOS}}^{(\text{iii})}$ read as

$$p_{\text{LOS}}^{(\text{i})} = 1-\mathcal{F}_{|h_{\text{SD}}|^2}\left(\frac{1}{P_{\text{S}}}k_0\right) \tag{38}$$

$$p_{\text{LOS}}^{(\text{ii})} = \int_{\frac{1}{P_{\text{S}}}k_1'}^{\frac{1}{P_{\text{S}}}k_0} f_{|h_{\text{SD}}|^2}(x)\left(1-\mathcal{F}_{\|\boldsymbol{h}_{\text{SR}}\|_2^2}\left(\frac{1}{P_{\text{S}}}k_0-x\right)\right)dx \tag{39}$$

$$p_{\text{LOS}}^{(\text{iii})} = \int_{0}^{\frac{1}{P_{\text{S}}}k_1'} f_{|h_{\text{SD}}|^2}(x)\left(1-\mathcal{F}_{\|\boldsymbol{h}_{\text{RD}}\|_2^2}\left(\frac{1}{P_{\text{R}}}(k_1'-P_{\text{S}}x)\right)\right)dx \tag{40}$$

with

$$k_0 = 2^{\rho}-1 \tag{41}$$

$$k_1' = \frac{2^{\rho-(N_{\text{R}}+1)\log_2\left(1+\frac{1}{\mu(N_{\text{R}}+1)}\right)}-1}{\mu(P_{\text{S}}+P_{\text{R}})}. \tag{42}$$

We are not aware of closed-form expressions for $p_{\text{LOS}}^{(\text{ii})}$ and $p_{\text{LOS}}^{(\text{ii})}$. Therefore, we apply numerical integration in our simulations.

VIII. Large Number of Antennas at the Relay

In this section, we assume a large number of antennas at the relay. By means of the Law of Large Numbers, we approximate the squared channel as follows

$$\|\boldsymbol{h}_{\text{RD}}\|_2^2\approx\|\bar{\boldsymbol{h}}_{\text{RD}}\|_2^2+\|\hat{\boldsymbol{h}}_{\text{RD}}\|_2^2\approx N_{\text{R}}\sigma_{\boldsymbol{h}_{\text{RD}}}^2 \tag{43}$$

$$\|\boldsymbol{h}_{\text{SR}}\|_2^2\approx\|\bar{\boldsymbol{h}}_{\text{SR}}\|_2^2+\|\hat{\boldsymbol{h}}_{\text{SR}}\|_2^2\approx N_{\text{R}}\sigma_{\boldsymbol{h}_{\text{SR}}}^2. \tag{44}$$

Consequently, the formulation of $R_{\text{DF}}^{(1)}$ in (6) can be approximated with a deterministic expression

$$R_{\text{DF}}^{(1)}(\beta)\approx\log_2\left(1+(1-g(\beta))\,N_{\text{R}}\sigma_{\boldsymbol{h}_{\text{SR}}}^2P_{\text{S}}\right). \tag{45}$$

As long as we assume coherent transmission, i.e., $\beta>0$, the approximations proposed in (43) and (44) are not applicable to the expression $R_{\text{DF}}^{(2)}$ in (7). Although, for the special case of $\beta=0$ and $\boldsymbol{R}_{\text{R}}=\frac{P_{\text{R}}}{N_{\text{R}}}\mathbf{I}$, the outage CSB expression in (10) and the DF outage rate in (9) are given in closed-forms as follows

$$C_{\text{CSB}}^{(\text{out})}\approx\log_2\left(1+P_{\text{S}}\mathcal{F}_{|h_{\text{SD}}|^2}^{-1}(\varepsilon)+\min\left\{P_{\text{S}}N_{\text{R}}\sigma_{\boldsymbol{h}_{\text{SR}}}^2,P_{\text{R}}\sigma_{\boldsymbol{h}_{\text{RD}}}^2\right\}\right) \tag{46}$$

$$R_{\text{DF}}^{(\text{out})}\approx\log_2\left(1+\min\left\{P_{\text{S}}N_{\text{R}}\sigma_{\boldsymbol{h}_{\text{SR}}}^2,P_{\text{R}}\sigma_{\boldsymbol{h}_{\text{RD}}}^2+P_{\text{S}}\mathcal{F}_{|h_{\text{SD}}|^2}^{-1}(\varepsilon)\right\}\right). \tag{47}$$

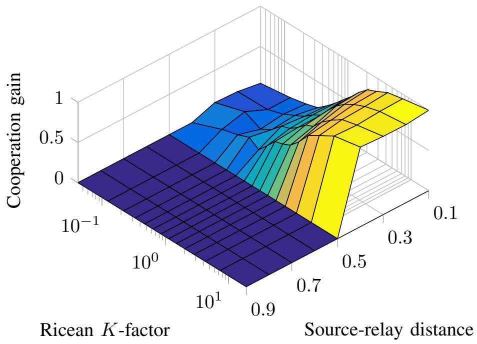

Fig. 2. Gain of source-relay cooperation with respect to the source-relay distance and the Rician K-factor for $\varepsilon = 0.25$

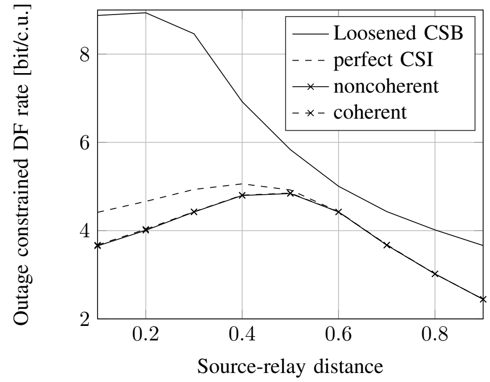

Fig. 3. Outage-constrained DF rates for source and single-antenna relay cooperating as well as for the non-coherent transmission. $K = 0.25, \varepsilon = 0.25$

This approximation is valid primarily for low values of the K-factor, i.e., when the channel's mean does not dominate. The channel is then "close" to Rayleigh for which non-coherent transmission is optimal [8].

We also note that for a sufficiently large number of relay antennas, the expressions in (46) and (47) are with high probability equal, i.e.,

$$C_{\text{CSB}}^{(\text{out})} \approx R_{\text{DF}}^{(\text{out})} \approx \log_2\left(1 + P_{\text{R}}\sigma_{\boldsymbol{h}_{\text{RD}}}^2 + P_{\text{S}}\mathcal{F}_{|h_{\text{SD}}|^2}^{-1}(\varepsilon)\right). \quad (48)$$

Therefore, as the upper and lower bound for the capacity are equal, this expression is the approximation of the channels' capacity in this special case. This case relates to the situation when (with high probability) the limiting factor for C_{CSB} and R_{DF} is $C_{\text{CSB}}^{(2)}$ and $R_{\text{DF}}^{(2)}$, respectively. Those expressions are equal [cf. (7)].

IX. Simulation Results

In our simulations, we evaluate the $\varepsilon-$outage-constrained DF rate for various setups. For the simulations, we use the line network model [8]. This means, that $\sigma_{\boldsymbol{h}}^2 = d^{-\alpha}$, where d is the distance between the respective terminals and we set arbitrarily $\alpha = 4$. For our simulations, we set the required outage probability ε to $\varepsilon = 0.25$.

Our Monte-Carlo simulations for single-antenna relay agree with our suggestions from Section IV. In Fig. 2, we show a 3D plot with the source-relay distance on the x-axis, the Rician K-factor on the y-axis and the benefit from cooperation on the z-axis. We define the cooperation gain as follows

$$\text{CG} = \frac{R_{\text{coh}}(\varepsilon) - R_{\text{non-coh}}(\varepsilon)}{R_{\text{perf. CSI}}(\varepsilon) - R_{\text{non-coh}}(\varepsilon)} \quad (49)$$

where the ε-outage-constrained DF rate is denoted by R and he subscripts refer to different choices of the variables β and r_{SR} (cf. Section IV). We see that for each relay position, decreasing K results in a decrease of the cooperation gain. We also see, that for large distances between the source and the relay, i.e., $d_{\text{SR}} > 0.5$, we get no benefit from cooperation. This is because the first rate expression in (11) becomes the main limiting factor in this region.

For single-antenna at the relay, Figures 3, 4, and 5 give an insight into the results for three values of the Rician K-factor, i.e., $K \in \{0.25, 1, 4\}$. We compare the outage-constrained DF rates when only the channel statistics are available at the transmitters [and r_{SR} is as in (15)] with two extreme cases. The first one assumes perfect CSI at the transmitters and, thus, r_{SR} as in (14). In the second one, non-coherent source-relay transmission is applied. Similarly as in Fig. 2, we see that gains from cooperation are possible only when the relay is close to the source, i.e., $d_{\text{SR}} \leq 0.5$. Moreover, the transmission profits from the knowledge of the channel statistics only if the channel mean is sufficiently strong, i.e., for higher values of K.

For multiple antennas at the relay ($N_{\text{R}} > 1$) and for high values of the Ricean K-factor, we expect that the system achieves better performance with rank–one $\boldsymbol{R}_{\text{R}}$ as in (19) since the channel mean is "close" to the channel itself. In contrast, for low values of K, we expect better results with the scaled identity $\boldsymbol{R}_{\text{R}}$ in (20). Figures 6, 7, and 8 agree with this suggestion. We also observe that the transmission profits from cooperation depending on the value of K similarly to the single-antenna setup. Moreover, compared to the single-antenna setup, the cooperation helps in the transmission for a larger range of d_{SR}, i.e., even for $d_{\text{SR}} = 0.5$.

In all the figures, we also plot the loosened CSB (cf. Section VII). As expected [13], it is loose if $d_{\text{SR}} < 0.5$ and tight otherwise. It is tighter for multiple antennas at the relay compared to the single-antenna case.

Figs. 9 and 10 give an additional insight into the impact of the β parameter on the outage-constrained DF rate. In Fig. 9, the outage-constrained DF rates for different values of β and different positions of the relay are presented. As expected (and explicitly shown in Fig. 10), the optimal value of β decreases with the distance between the source and the relay. From the shape of the curves in Fig. 9, we can also draw the conclusion, that inaccuracies in the choice of optimal β does not affect severely the outage-constrained rates.

X. Conclusions

We analyzed the influence of the source-relay cooperation on the outage-constrained capacity of the relay channel. The

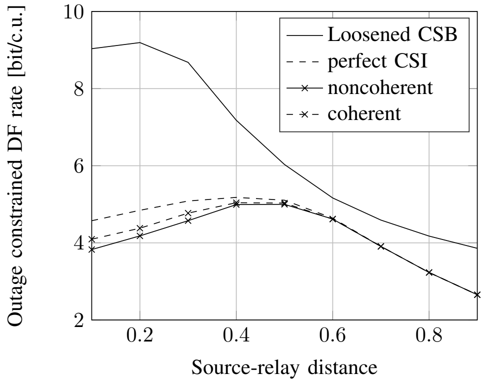

Fig. 4. Outage-constrained DF rates for source and single-antenna relay cooperating as well as for the non-coherent transmission. $K = 1, \varepsilon = 0.25$

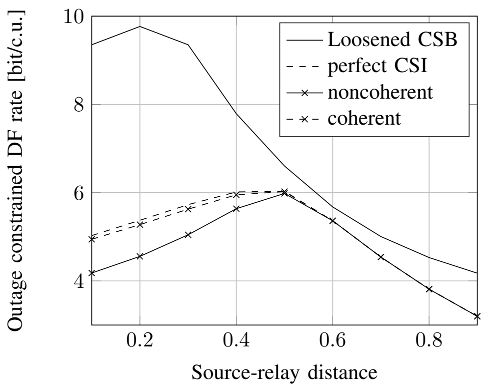

Fig. 5. Outage-constrained DF rates for source and single-antenna relay cooperating as well as for the non-coherent transmission. $K = 4, \varepsilon = 0.25$

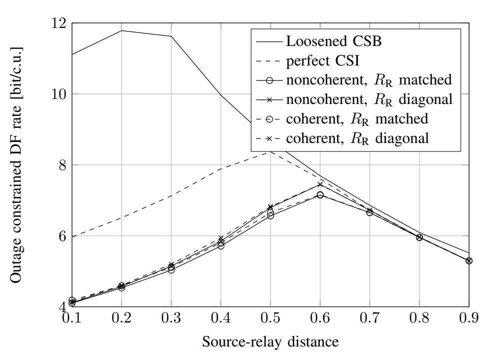

Fig. 6. Outage-constrained DF rates for source and (multi-antenna) relay cooperating as well as for the non-coherent transmission. $K = 0.25, \varepsilon = 0.25, N_R = 4$

study has considered the Rician channel and multiple antennas at the relay terminal. We have identified setups where the source-relay cooperation provides particularly high gains. We have also proposed and evaluated heuristic ways of constructing the $\boldsymbol{r}_{SR}$ vector carrying specifics of the source-relay cooperation, as well as the relay covariance matrix $\boldsymbol{R}_R$.

Additionally, we have extended the upper bound for the CSB, namely loosened CSB (cf. [13]) to the Rician channel

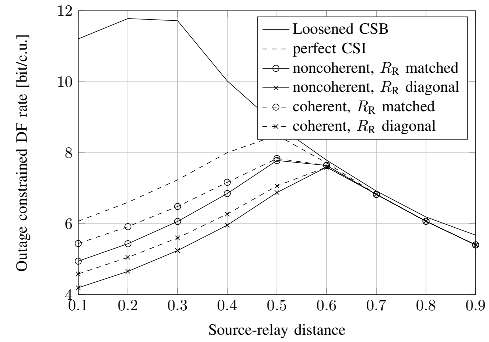

Fig. 7. Outage-constrained DF rates for source and (multi-antenna) relay cooperating as well as for the non-coherent transmission. $K = 1, \varepsilon = 0.25, N_R = 4$

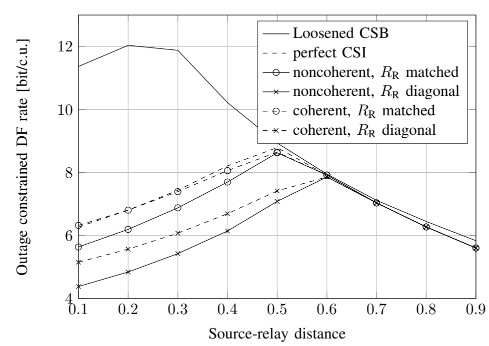

Fig. 8. Outage-constrained DF rates for source and (multi-antenna) relay cooperating as well as for the non-coherent transmission. $K = 4, \varepsilon = 0.25, N_R = 4$

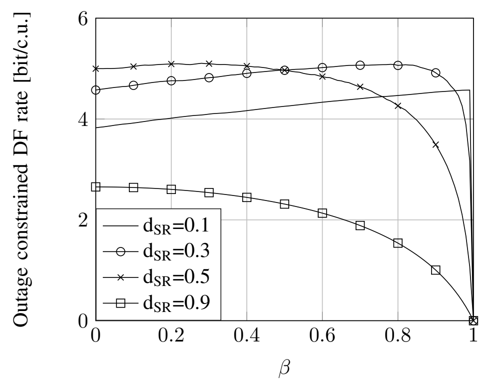

Fig. 9. Outage-constrained DF rates for different degrees of cooperation (β) for various relay positions. $K = 1, \varepsilon = 0.25, N_R = 1$

model and multiple antennas at the relay terminal. Moreover, we provided analytical approximations for the outage-constrained DF rates.

Finally, we have analyzed the setup with very high number of antennas at the relay terminal.

Appendix

A. PDF's and CDF's of the Squared Channel 2-Norms

For the Rician channel model, the PDF's and CDF's of the random variables $\|\boldsymbol{h}_{SR}\|_2^2$, $\|\boldsymbol{h}_{RD}\|_2^2$, and $|h_{SD}|^2$ have closed

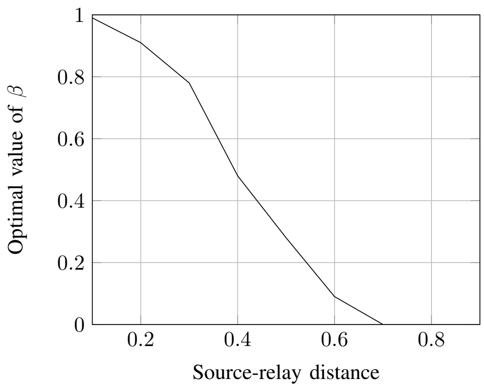

Fig. 10. The optimal choice of β dependent on the relay position. $K = 1, \varepsilon = 0.25, N_{\mathrm{R}} = 1$

form representations. Omitting the subscripts referring to the links, they can be expressed with the PDF's and CDF's for the non-central chi-squared distribution as follows

$$f_{\|\boldsymbol{h}\|_2^2}(x) = \frac{2}{\sigma^2_{\hat{\boldsymbol{h}}}} f_{\chi^2_{2l(\boldsymbol{h})}(\lambda)}\left(\frac{2}{\sigma^2_{\hat{\boldsymbol{h}}}}x\right), \tag{50}$$

$$\mathcal{F}_{\|\boldsymbol{h}\|_2^2}(y) = \mathcal{F}_{\chi^2_{2l(\boldsymbol{h})}(\lambda)}\left(\frac{2}{\sigma^2_{\hat{\boldsymbol{h}}}}y\right) \tag{51}$$

where the non-centrality parameter reads as $\lambda = 2\|\bar{\boldsymbol{h}}\|_2^2/\sigma^2_{\hat{\boldsymbol{h}}}$ and $l(\boldsymbol{h})$ denotes the length of the channel vector.

REFERENCES

[1] E. van der Meulen, "Three-Terminal Communication Channels," *Advances in Applied Probability*, vol. 3, no. 1, pp. 120–154, 1971.

[2] T. Cover and A. Gamal, "Capacity theorems for the relay channel," *IEEE Transactions on Information Theory*, vol. 25, no. 5, pp. 572–584, Sep. 1979.

[3] U. Madhow, *Fundamentals of Digital Communication*. Cambridge University Press, 2008.

[4] G. Kramer, M. Gastpar, and P. Gupta, "Cooperative Strategies and Capacity Theorems for Relay Networks," *IEEE Transactions on Information Theory*, vol. 51, no. 9, pp. 3037–3063, Sep. 2005.

[5] A. Hø st Madsen and J. Zhang, "Capacity bounds and power allocation for wireless relay channels," *IEEE Transactions on Information Theory*, vol. 51, no. 6, pp. 2020–2040, June 2005.

[6] A. Avestimehr and D. Tse, "Outage capacity of the fading relay channel in the low-snr regime," *IEEE Transactions on Information Theory*, vol. 53, no. 4, pp. 1401–1415, Apr. 2007.

[7] J. Gomez-Vilardebo and A. Perez-Neira, "Upper bound on outage capacity of orthogonal relay networks," in *IEEE 7th Workshop on Signal Processing Advances in Wireless Communications, 2006. SPAWC '06.*, July 2006, pp. 1–5.

[8] A. Gründinger, L. Gerdes, M. Joham, and W. Utschick, "Bounds on the outage constrained capacity of the single-antenna gaussian relay channel," in *2015 49th Annual Conference on Information Sciences and Systems (CISS)*, Mar. 2015, pp. 1–6.

[9] L. Gerdes and W. Utschick, "Optimized capacity bounds for the MIMO relay channel," in *2011 IEEE International Conference on Acoustics, Speech and Signal Processing (ICASSP)*, May 2011, pp. 3336–3339.

[10] J. P. Imhof, "Computing the distribution of quadratic forms in normal variables," *Biometrika*, vol. 48, no. 3-4, p. 419426, Dec 1961.

[11] H. Liu, Y. Tang, and H. H. Zhang, "A new chi-square approximation to the distribution of non-negative definite quadratic forms in non-central normal variables," *Computational Statistics and Data Analysis*, vol. 53, no. 4, p. 853856, Feb 2009.

[12] J. Kiefer, "Sequential Minimax Search for a Maximum," *Proceedings of the American Mathematical Society*, vol. 4, no. 3, p. 502506, 1953.

[13] A. Gründinger, L. Gerdes, M. Joham, and W. Utschick, "Bounds on the Outage Constrained Capacity of the Gaussian Relay Channel," in *Communications in Interference Limited Networks*, W. Utschick, Ed. Springer, 2016.

[14] A. Gamal and Y. Kim, *Network Information Theory*. Cambridge University Press, 2011. [Online]. Available: https://books.google.co.uk/books?id=l31D4DU7jykC